npg

OUTSTANDING OBSERVATION

Fetal *Hox11* expression patterns predict defective target organs: a novel link between developmental biology and autoimmunity

Anna Lonyai[1], Shohta Kodama[2], Douglas Burger[1] and Denise L Faustman[1]

Developmental biology has long been ignored in the etiology and diverse manifestations of autoimmune diseases. Yet a role for development is suggested by intriguing overlaps in particular organs targeted in autoimmune diseases, in this case type 1 diabetes and Sjogren's syndrome. Patients with type 1 diabetes have high rates of co-occurring Sjogren's syndrome, and both conditions are associated with hearing loss and tongue abnormalities. All of these co-occurrences are found in organs tracing their lineage to the developmental transcription factor *Hox11*, which is expressed in embryonic cells destined for the pancreas, salivary glands, tongue, cranial nerves and cochlea. To determine whether development contributes to autoimmunity, we compared four target organs in NOD mice (an animal model for type 1 diabetes and Sjogren's syndrome) with NOD-SCID mice (which lack lymphocytes) and normal controls. We examined the structure and/or function of the cochlea, salivary glands, pancreas and tongue at early time points after birth. Before the usual time of the onset of type 1 diabetes or Sjogren's syndrome, we show that all four *Hox11*-derived organs are structurally abnormal in both NOD mice and NOD-SCID mice versus controls. The most striking functional defect is near complete hearing loss occurring before the normal time of the onset of autoimmunity. The hearing loss is associated with severe structural defects in the cochlea, suggesting that near-deafness occurs independent of autoimmune attack. The pancreas and salivary glands are also structurally abnormal in NOD and NOD-SCID mice, but they are functionally normal. This suggests that autoimmune attack of these two organs is required for functional failure. We conclude that a developmental lineage of cells contributes to autoimmunity and predicts which organs may be targeted, either structurally and/or functionally. Taken together, our findings challenge the orthodoxy that autoimmunity is solely caused by a defective immune system.
Immunology and Cell Biology advance online publication, 26 February 2008; doi:10.1038/icb.2008.6

For decades, the prevailing view held by immunologists has been that autoimmune diseases are solely caused by a defective immune system that targets self-antigens on self tissues. Support for this dogma arose from classic experiments in the nonobese diabetic (NOD) mouse, a commonly used model of autoimmune-mediated destruction of the pancreas and salivary glands, resulting in type 1 diabetes and a Sjogren's syndrome, respectively. NOD mice with a hampered immune system (NOD-SCID) fail to mount an autoimmune attack on pancreatic insulin secreting cells (type 1 diabetes) or on salivary glands (Sjogren's syndrome).[1–3] Immune attack on multiple organs in the same animal commonly has been explained by epitope spreading, the concept that fortuitous cross-reactivity between a particular epitope on one tissue matches a similar tissue epitope. This causes the immune system response to 'cross react' and target diverse organs. While an altered immune response has been considered the primary culprit of autoreactivity, a recent study has begun to explore the indirect contribution of sensory neurons to β-cell dysfunction in the pathophysiology of type 1 diabetes in NOD mice.[4]

Multi-organ attack by a deranged autoimmune system is a common theme for type 1 diabetes and Sjogren's syndrome in NOD mice and humans.[5–14] For example, 80–90% of NOD mice in most colonies exhibit type 1 diabetes and Sjogren's syndrome (Table 1). In humans, some epidemiological studies reveal that up to 55 percent of patients with type 1 diabetes exhibit co-occurring Sjogren's syndrome (Table 1).[15] The cochlea and tongue are also frequently targeted in humans and, as systematically reported here for the first time, in NOD mice. To our knowledge, this is an early report to explain this co-occurrence by examining the direct contribution of a specific lineage of stem cells that govern the range of organs selected for autoimmune attack and dysfution.

[1]Immunobiology Laboratories, Massachusetts General Hospital and Harvard Medical School, Charlestown, MA, USA and [2]Tissue Engineering and Regenerative Medicine, Brigham and Women's Hospital, Harvard Medical School, Boston, MA, USA
Correspondence: Dr DL Faustman, Immunobiology Laboratories, Massachusetts General Hospital and Harvard Medical School, Building 149, 13th Street, Room 3602, Charlestown, MA 2129, USA.
E-mail: faustman@helix.mgh.harvard.edu

Table 1 Epidemiological co-occurrence of autoimmune diseases or other abnormalities in humans and NOD mouse in *Hox11*-expressing organs[a]

Illness	Illness/defect	Co-occurrence (%)	Reference(s)
HUMANS			
Type 1 diabetes	Sjogren's syndrome or symptoms	25–55	15
Sjogren's syndrome	Hearing loss	5–46	16,17
Sjogren's syndrome	Tongue/taste abnormalities	>80	21
Type 1 diabetes	Hearing loss	11–90	18,19,37
Type 1 diabetes	Tongue abnormalities	12	20
MICE			
NOD mouse			
Type 1 diabetes	Sjogren's syndrome	80–90	38
Sjogren's syndrome	Hearing loss	>95	This article
Sjogren's syndrome	Tongue abnormalities	>90	This article
Type 1 diabetes	Hearing loss	>95	This article
Type 1 diabetes	Tongue abnormalities	>90	This article

[a]Some disease occurrence rates were affected in mouse strains by the sex of the cohort. This table reports the data from the male or female animals with the higher expression of the disease if there is a sex difference in disease penetrance. Also due to limitations in table size, the authors acknowledge that the mouse diseases that mimic human disease should be referred to as 'type I diabetes like' or 'Sjorgren's syndrome like.'

Hearing loss in humans with Sjogren's syndrome has been interpreted not as a primary manifestation of the syndrome but as a secondary consequence of immune attack. But this view does not fit with the following clinical observations: hearing loss in patients having Sjogren's syndrome is not related to disease duration, considering that it can occur early in the presentation of salivary gland disease. Also, it is not associated with salivary gland disease severity, extraglandular manifestations or concentrations of autoantibodies.[16,17] Hearing loss in humans with type 1 diabetes also occurs,[18] yet it has been interpreted as secondary to severe vascular-mediated damage from long-standing elevated blood sugar levels. This seems to be a reasonable hypothesis because altered auditory thresholds are related to age and disease duration. Yet, a recent study remarkably showed cochlear changes in patients with type 1 diabetes that mirror, in many aspects, the same structural abnormalities that we subsequently identify here in NOD mice.[19] Finally, a large longitudinal study of oral health of type 1 diabetic patients surprisingly reveals that the tongue exhibits altered gross soft-tissue morphology suggestive of a developmental defect.[20] Taste is also altered in Sjogren's syndrome,[21] and, not surprisingly, it is partially controlled by cranial nerves, which also trace their lineage to *Hox11*, a developmental transcription factor. While other examples of co-occurring autoimmune diseases and/or manifestations exist in separate animal models of autoimmunity (for example, lupus co-occurring with Sjogren's syndrome and hearing loss in other mouse strains[22–24]), the focus here is on understanding the etiological reasons behind co-occurring organ abnormalities in type 1 diabetes and Sjogren's syndrome, along with two frequently associated conditions, hearing loss and morphological abnormalities of the tongue.

We hypothesized that the puzzling epidemiological and clinical overlaps could be explained by a common developmental lineage of the four affected organs. That lineage may trace to stem cells expressing the developmental transcription factor, *Hox11*. The *Hox11/Tlx1* gene and closely related family members *Hox11L1/Tlx2* and *Hox11L2/Tlx3* form a group of homeodomain genes involved in the development of central nervous system and of specific peripheral organs and tissues. The *Hox* gene family is highly conserved over a broad range of species, such as zebrafish, chicks, *Xenopus* and mammals.[25–30] In zebrafish embryos, *Hox11* family members participate in early differentiation of the nervous system and cranial sensory ganglia.[25] In chick embryos, *Hox11* is expressed in cranial sensory ganglia in the hindbrain and may purportedly play a role in the differentiation and survival of specific neurons and neuronal circuitry.[26] In *Xenopus*, *Hox11* expression is localized to the brachial arches, cranial sensory ganglia and the spinal cord.[27]

The role of *Hox11* genes in the development of the mammalian nervous system is similar to that of lower species, but *Hox11* is also expressed in certain peripheral organs and tissues. *Hox11* transcripts are detected in mice at E8.5 (day 8.5 in embryonic development) on the surface ectoderm and central mesenchyme of the first brachial arch, which later forms the tongue, tooth primordial, pharynx, inner ear and spleen.[28,31,32] By day E12.5–E15.5, *Hox11* expression is observed in the developing pancreas and salivary glands and is also localized to certain cranial nerves, such as the vestibulocochlear nerve (VIII);[31] portions of the spinal cord and curvature of the pons-medulla also robustly express *Hox11* during this fetal stage. Deletion of multiple *Hox* gene family members, but not sole deletion of *Hox11*, typically results in multiple organ afflictions. Taken together, these findings are consistent with wide-ranging roles for the *Hox* gene family in neuronal and mesodermal cell migration during development of the mammalian embryo. Although the *Hox* gene family is most active before birth, after which its activity has been thought to cease, we recently reported that adult NOD mice[33] and adult humans[34] possess active *Hox11* transcripts in a population of adult stem cells that is uniquely expressed in the spleen—but not in other organs.

In NOD mice, type 1 diabetes develops spontaneously between 22–30 weeks of age. Early signs of Sjogren's syndrome, assessed by slowing of salivary function, can be measured earlier, at 14–20 weeks of age. From birth and before the onset of detectable autoimmune destruction of the pancreas and salivary glands, young NOD mice display structural abnormalities in *Hox11*-derived tissues.[1–3,35] Specifically, before weaning at 4–5 weeks of age, the pancreas in NOD mice contains immature, poorly shaped, insulin-secreting islet clusters. As NOD mice age, these islets become very large and possess an irregular shape, relative to control mice.[1,2,35] NOD mice shortly after weaning also have abnormally formed salivary glands, including the selective loss of acinar tissue and more numerous secretary glands, relative to controls.[3]

Here, we explore whether overlapping autoimmune failures in several organs are linked to a shared developmental lineage tracing to *Hox11* stem cells. We examine the structure and/or function of the cochlea, salivary glands, pancreas and tongue at early time points after birth in three groups of mice. Any similarities between NOD mice and NOD-SCID mice (relative to controls) found before usual time of the onset of spontaneous autoimmunity suggest a primarily developmental origin, rather than an immunological origin, of autoimmunity.

RESULTS

Hox11 derivative tissues uniformly show structural abnormalities in NOD and NOD-SCID mice

Here, we first sought to confirm earlier findings—most importantly the finding that structural abnormalities occur before autoimmune-mediated organ dysfunction of the pancreas and salivary glands. We compared NOD, NOD-SCID and normal controls (C57BL/6) at 5–8 weeks of age. NOD-SCID mice differ from NOD mice by a single genetic mutation (SCID) that interrupts the immune system and, thus, tissue destruction from autoimmune-mediated disease. We found that young NOD mice, in comparison with controls, display structural abnormalities in the pancreas and salivary glands, in agreement with previous investigators (Figures 1 and 2, Table 2). NOD-SCID mice exhibit the same structural abnormalities as NOD mice in the shape and numbers of pancreatic islets and in the shape of the ductal structures in the salivary glands, relative to the control C57BL/6 mice. Pancreatic islets from NOD as well as NOD-SCID mice displayed statistically more immature islets, as reflected by the small size and apparently more numerous individual islets per tissue cross-section, than did the C57BL/6 mice (Figures 1 and 2). Likewise, the salivary glands of NOD-SCID mice contain a high concentration of ductal to acinar tissue, as previously noted (Figures 1 and 2). This altered morphology was discernable on histological examination of hematoxylin- and eosin-stained fixed tissue. Finding similar structural defects in NOD and NOD-SCID mice suggests that the abnormalities are occurring independent of the immune system.

Next, we examined the morphology of the tongue at 5–8 weeks of age (Figures 1g–i). The rationale for examining the tongue is not only the epidemiological relationship in humans, but also the finding that, during development, localized expression of *Hox11* on the surface of the ectoderm and presumptive myoblasts of mesoderm origins is consistent with the notion that the Hox11 protein marks subpopulations of cells destined to give rise to components of the tongue. This hypothesis is also supported by the observation that at E9.5, *Hox11* expression in surface ectoderm condenses at the ventral midline, which forms the median sulcus and surface ectoderm of the tongue.[31] Therefore, to further substantiate the hypothesis that additional *Hox11*-derived tissues are malformed in NOD mice, we examined the tongues of NOD, NOD-SCID and C57BL/6 mice. As shown in Figure 1, both the NOD and the NOD-SCID tongues displayed detectable histological abnormalities, relative to the C57BL/6 controls, especially in the fungiform papillae, which are mushroom-like structures for taste that appear visually as small, broad and flat entities on the surface of the tongue. Statistical analysis of the ratio of the number of fungiform papillae to the total number of papillae (fungiform and filiform) in NOD and NOD-SCID versus control mice showed a statistically significant higher ratio of fungiform papillae to total papillae (Figure 2e). This difference resulted from an overabundance of fungiform papillae and a relative reduction in the total number of nonfungiform papillae in both NOD and NOD-SCID mice compared with controls.
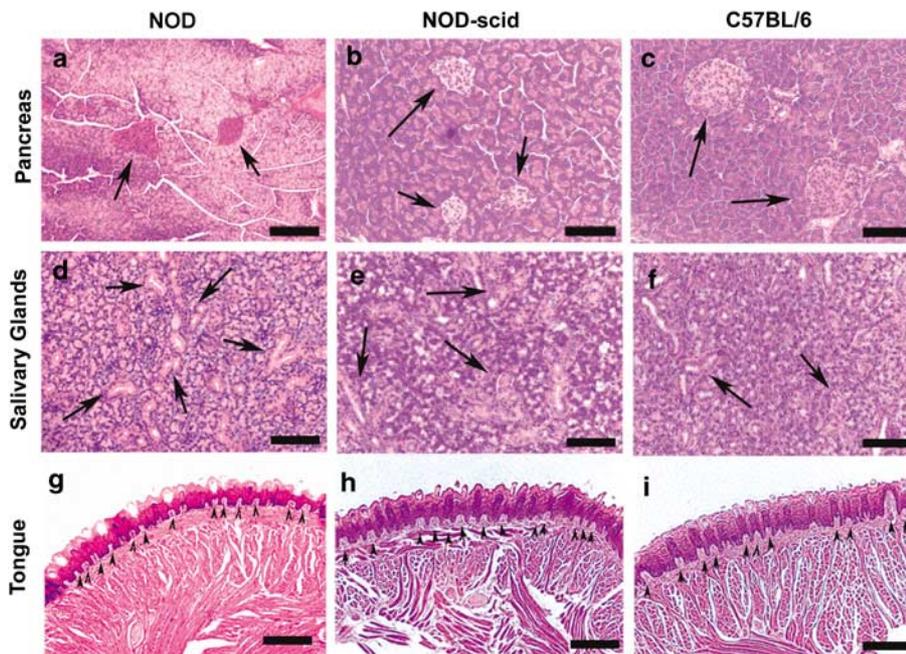

Figure 1 Comparison of different *Hox11*-lineage tissues (pancreas, salivary glands, tongue) in NOD, NOD-SCID and C57BL/6 mice. (**a**–**c**) Smaller but more prevalent islets (arrows) in the pancreas of a young 5- to 8-week-old NOD (**a**) and NOD-SCID mouse (**b**) compared to age-matched C57BL/6 mouse (**c**), shown at ×20 magnification with scale bars signifying 100 μm. (**d**–**f**) Higher ductal (arrows) to acinar tissue ratio in the NOD (**d**) and NOD-SCID mouse (**e**) salivary glands compared with the C57BL/6 mouse (**f**), shown at ×20 magnification with scale bars signifying 100 μm. The acinar tissue is that which surrounds the ductal tissue. (**g**–**i**) High concentration of fungiform papillae (arrowhead) in the tongue of a NOD (**g**) and NOD-SCID (**h**) mouse compared to the C57BL/6 mouse (**i**), shown at ×10 magnification with scale bars signifying 200 μm. (**a**–**i**) All sections were hematoxylin and eosin stained.
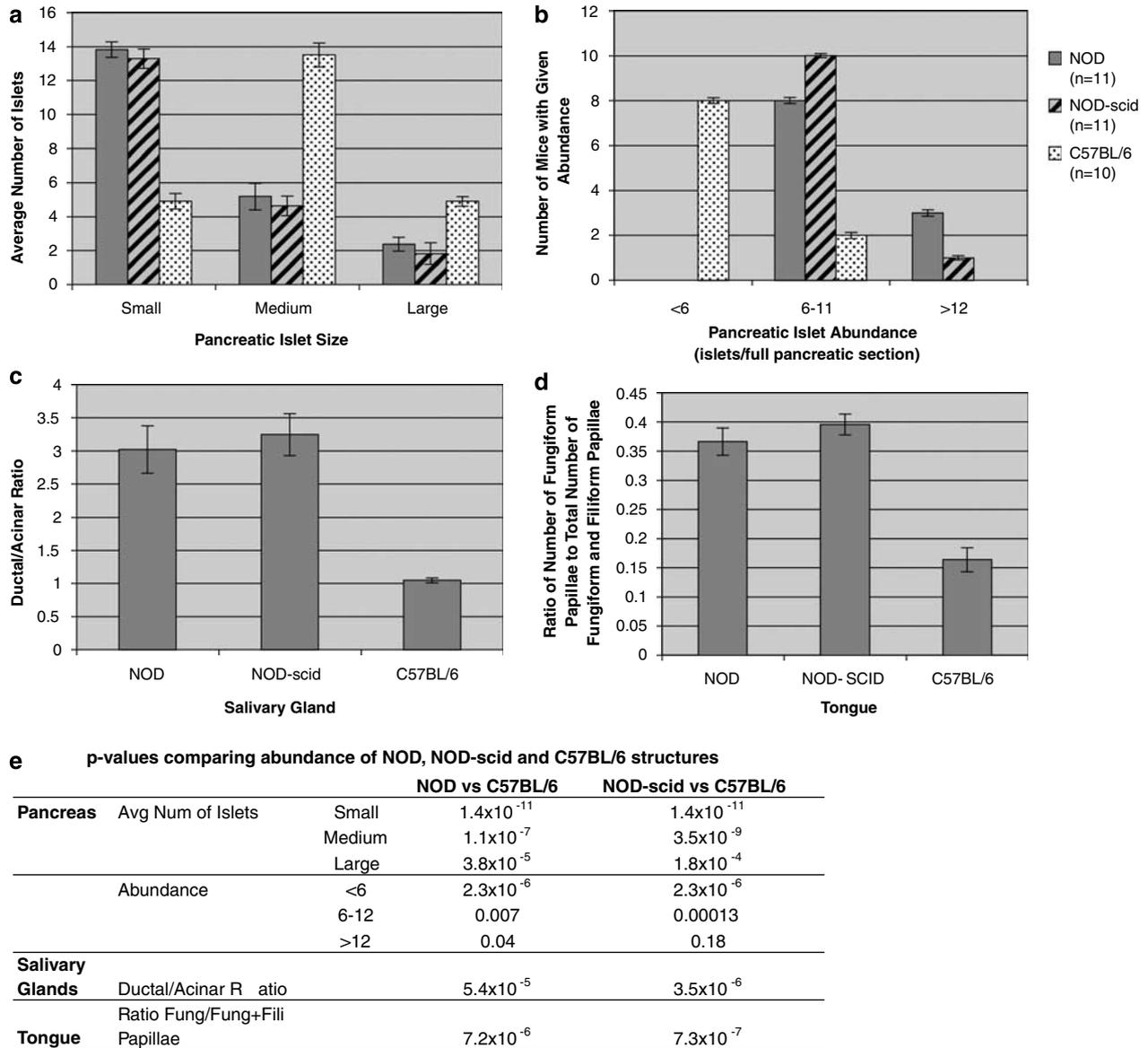
Figure 2 Quantitative comparisons of pancreatic islets (**a** and **b**), salivary glands (**c**) and tongue morphology between NOD, NOD-SCID and C56BL/6 mice. A statistically greater number of small pancreatic islets were present in NOD ($n=11$) and NOD-SCID ($n=11$) mice compared to C57BL/6 mice ($n=10$) and a statistically increased abundance of salivary gland ductal glands per acinar tissue in both NOD ($n=11$) and NOD-SCID ($n=11$) mice when compared to the control C57BL/6 ($n=9$) mice. The numbers of fungiform papillae to total numbers of fungiform and filiform papillae were elevated in both NOD ($n=8$) and NOD-SCID ($n=7$) mice compared with the C57BL/6 tongues ($n=8$). The varying animals groups were compared (NOD vs control, and NOD-SCID vs control) for each of the tissues and the tissue morphology per mouse strain using a *t*-test assuming equal variances (**e**). All *P*-values were significant (<0.05), except for the NOD-SCID and C57BL/6 in the number of samples that had more than 12 pancreatic islets.

Hox11 derivative cochlear structures are also abnormal in NOD and NOD-SCID mice

Next, we conducted histological studies of the cochlea across the three groups of animals at 5–8 weeks of age, a time before the typical onset of immune-mediated disease. We revealed clearly visible structural abnormalities in the cochlea of the inner ear in NOD and NOD-SCID mice, relative to C57BL/6 control mice (Figure 3, Table 2). The structures affected by the developmental abnormalities were nearly identical in NOD and NOD-SCID mice. Specifically, we observed a lack of development of the cells in the spiral ligament (Figures 3d and e) without a change in the number of cochlear turns, relative to controls. Also evident were poorly formed spiral ganglion, with

primarily Schwann cell nuclei (Figures 3b and c). This defect was uniformly observed in all NOD mice and less frequently observed in NOD-SCID mice (Figure 3h). Furthermore, the organ of Corti in the NOD animals appeared altered, containing less than half the number of inner hair cells apparent in control organs as well as an apparent failure to form the organ of Corti canals in some of the mice (Figures 3f and g). Other structural defects were also observed, such as deterioration in the stria vascularis and the spiral limbus of the lower second turn, but both of these defects had a low penetrance. No evidence of lymphocytic infiltration—a sign of immune-mediated disease—was observed in the altered cochlear structures and thus could not account for the observed histological aberrations and

Table 2 Abnormalities in *Hox11* derivative tissues

	Abnormal cell structures mouse strains			Organ malfunction mouse strains		
	NOD	NOD-SCID	Control C57	NOD	NOD-SCID	Control C57
					Deafness[a]	
Cochlea/ear	Abnormal	Abnormal	Normal	Abnormal	Abnormal	Normal
	100%	100%	<22%	100%	100%	0%
	n=13	n=10	n=8	n=13	n=10	n=8
					Diabetes[b]	
Pancreas	Abnormal	Abnormal	Normal	Abnormal	Normal	Normal
	100%	100%	0%	>85%	0%	0%
	n=15	n=18	n=18	n=56	n=15	n=15
					Salivary flow[c]	
Salivary gland	Abnormal	Abnormal	Normal	Abnormal	Normal	Normal
	100%	100%	0	>90%	0%	0%
	n=8	n=9	n=8	n=5	n=5	n=14
Tongue	Abnormal	Abnormal	Normal	NA	NA	NA
	100%	100%	100%			
	n=6	n=2	n=4			

Abbreviation: NA, not applicable.
Control mice in this study were C57BL/6 mice, sex and age matched to the NOD and NOD-SCID.
All cell structure comparisons in this table represent mice at 5–8 weeks of age.
[a]Hearing was monitored by ABR as described in the Methods at 5–8 weeks of age.
[b]Incidence of diabetes was monitored in female mice from about 15 weeks of age until diabetes, typically at 25 weeks of age.
[c]Salivary flow was monitored in mice after 12 weeks of age by the pilocarpine salivary flow test.

functional loss of hearing. This confirms that the hearing loss and structural abnormalities of the inner ear are primary defects unrelated to a direct cell-mediated immune attack.

Severe hearing loss exists in both NOD and NOD-SCID mice
Next, we examined hearing function, drawing upon several lines of evidence implicating the possibility of dysfunction. Not only there is an epidemiological relationship between hearing loss and the two conditions, Sjogren's and type 1 diabetes (Table 1), but *Hox11* expression is also tightly regulated in the central nervous system as it contributes to the development of both inner ear and cranial nerve, including the vestibulocochlear nerve and ganglion. Additional evidence supports the testing of hearing loss in NOD animals, which has heretofore not been undertaken. A past behavioral study revealed altered startle reflexes in NOD mice relative to controls, a finding that is consistent with hearing impairment.[36] We measured hearing function electrophysiologically using auditory brainstem responses (ABRs) in NOD, NOD-SCID and C57BL/6 control mice at 5–8 weeks of age. All 13 NOD mice had significantly higher thresholds with ABR testing than did the control mice. This result was indicative of severe hearing loss (Figure 4a). Half of the NOD animals had no measurable hearing at any of the frequencies tested (from 5 to 40 kHz). In the other animals, all had thresholds at or above 70 dB at all frequencies tested (see Supplementary Figure 1a). Thus, all NOD animals suffered from significant hearing loss, even at very young adult ages. Autoimmune diabetes in these animals typically presents as high blood sugar levels after 16 weeks of age. Therefore, the significant hearing loss in the NOD mice occurred before the onset of autoimmune disease in the animals. The lymphocytic inactivation of the immune system in the NOD-SCID strain did not rescue the animals from the near complete hearing defect (Figure 4b). All 10 NOD-SCID mice at 5–8 weeks of age had measurably higher ABR

thresholds compared to age-matched control mice (see Supplementary Figure S1b). Therefore, the presence or absence of an immune system had no measurable impact on the early onset and near complete hearing loss observed in NOD and NOD-SCID mice (Table 2).

DISCUSSION
Our current findings support the conclusion that a shared developmental pathway contributes to the etiology of at least some forms of autoimmune disease. This is one of the first reports to conclude that developmental defects in fetal *Hox11* derivative tissues identify later primary or, in some cases, secondary organ and tissue failure in adult mice. At least in the NOD model, developmental expression of *Hox11* predicts which organs and tissues will develop primary failures and/or structural abnormalities. Also some of the structural defects result in functional defects that apparently occur largely independent of secondary damage from immune-mediated disruptions (Table 2). Our observations of underlying developmental defects in *Hox11*-derived organs in NOD mice may apply to humans, given the similarities between animal and epidemiological studies of auto-immune diabetes and Sjogren's syndrome. Future human studies could enrich our understanding of immune diseases linked to altered fetal development.

Although *Hox11* is widely expressed in embryonic tissues, the mechanism by which *Hox11* predicts, at least in the NOD model, abnormal alterations in its more differentiated progeny—pancreatic islets, salivary glands, cochlear nerve and tongue—is not understood. But there are intriguing hints from previous experimental studies. A variety of studies suggest a linkage between the nervous and endocrine systems in type 1 diabetes. One of the primary autoantibodies indicative of β-cell death is glutamic acid decarboxylase (anti-GAD), a shared neural antigen of both pancreatic islets and neurons. GAD is considered one of the primary autoantibodies of human diabetes.
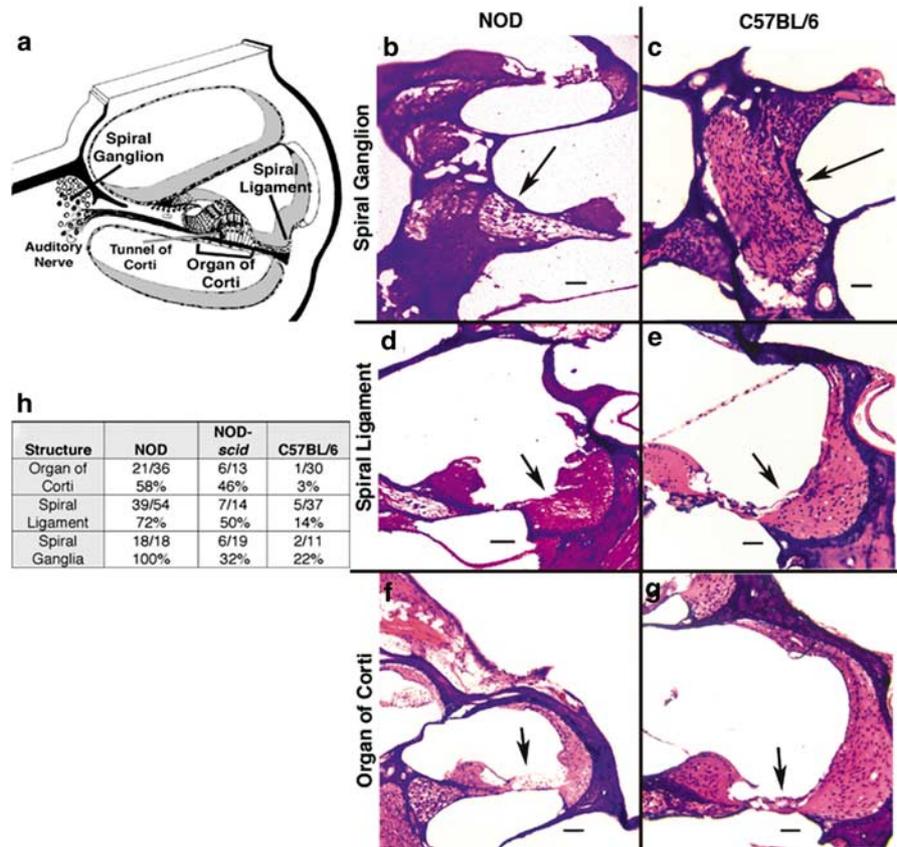
Figure 3 Comparison of NOD and C57BL/6 cochlear structures. (**a**) A schematic area of interest in the cochlea. (**b**–**g**) Histological cross-sections of the mouse cochlea were processed and cochlear structures were compared between NOD and C57BL/6 animals at 5–8 weeks of age. Structural abnormalities were found in the spiral ganglion, spiral ligament and organ of Corti in the NOD mice. (**b** and **c**) The spiral ganglion cells of the NOD mouse were greatly deteriorated (arrow, **b**), relative to the C57BL/6 control (arrow, **c**), with only the Schwann cell nuclei remaining. (**d** and **e**) There was also atrophy of the spiral ligament, as seen by the loss of cells in the NOD specimen (arrow, **d**), which is in sharp contrast to the fully populated spiral ligament in the control (arrow, **e**). (**f** and **g**) The organ of Corti of the NOD specimen appeared to be deteriorated and to have many fewer cells (arrow, **f**), including hair cells, compared to the control (arrow, **g**). Defects similar to those observed in the NOD cochlea were present in the NOD-SCID cochlea as well. (**b**–**g**) All sections were hematoxylin and eosin stained and all images taken at ×20 magnification. Scale bars: 100 μm. (**h**) Table showing the rate of abnormalities in the cochlear structures of NOD ($n=13$), NOD-SCID ($n=11$) and C57BL/6 ($n=8$) mice. Both the NOD and NOD-SCID mice exhibited a much higher rate of abnormality in the organ of Corti than did the C57BL/6 control, where abnormal was considered more than 50% loss of cells or if the structure had not developed properly, most commonly failing to form the tunnel of Corti. There was also a much higher rate of abnormality in the spiral ligament in the NOD and NOD-SCID mice, relative to the control, with abnormal showing at least 50% cell loss. All spiral ganglia were abnormal in the NOD mice (compared to a lower rate of abnormality in the NOD-SCID mice), where abnormal was considered at least a 50% neuron loss. Multiple turns in the cochlea were evaluated.

In *Drosophila*, there also appears to be during development an integrated neuron and islet system tracing to a common ancestral neuron in the brain.[39] Relatedly, manipulated NOD mice through blocking the costimulatory CD28/B7-2 or IL-2 pathways, have induced peripheral neuropathies.[40,41] Furthermore, in NOD mice, genetic ablation of sensory neurons through the *TRPV1* gene, which is expressed in sensory neurons prevents subsequent islet disease.[4] Therefore, both developmental biology and other types of studies suggest a neuro-endocrine link.

This study establishes that the examined *Hox11* derivative tissues have structural abnormalities. Could the *Hox11* gene itself, which produces a transcription factor, directly contribute to disease, or does *Hox11* merely mark tissues of a given lineage associated with subsequent autoimmune disease? *Hox11* (*Tlx1*) with its homeobox gene partner *Tlx3* are the first transcription factors required for the specification of glutantergic versus GABAergic neurons expressing GAD, the autoantigen in diabetes. *Hox11* expression selects

glutamatergic over GABAergic cell fate.[42] Therefore, it is anticipated that the dysfunction of *Hox11* signalling pathway or gene regulation could influence expression of GAD, thus altering the balance of GAD-expressing neurons, the ratios of excitatory and inhibitory neurons and perhaps exposures of the immune system to GAD. This alteration may contribute to the pathophysiology of type 1 diabetes by altered cell fate through yet to be determined altered regulatory steps.

What are the implications to future autoimmune therapies if the etiologic basis of autoreactivity is dictated by altered development of the target organ? In this model of autoimmunity, underlying developmental defects in *Hox11*-derived tissues makes them particularly susceptible to primary or secondary failure from immune-mediated destruction. Many new autoimmune therapies in development strive to remove or inactivate autoimmune cells to permit organ rescue and even organ regeneration. In the NOD model, targeted immune therapy might be beneficial for both the salivary glands and the pancreas for recovery or regeneration. For instance, NOD-SCID mice
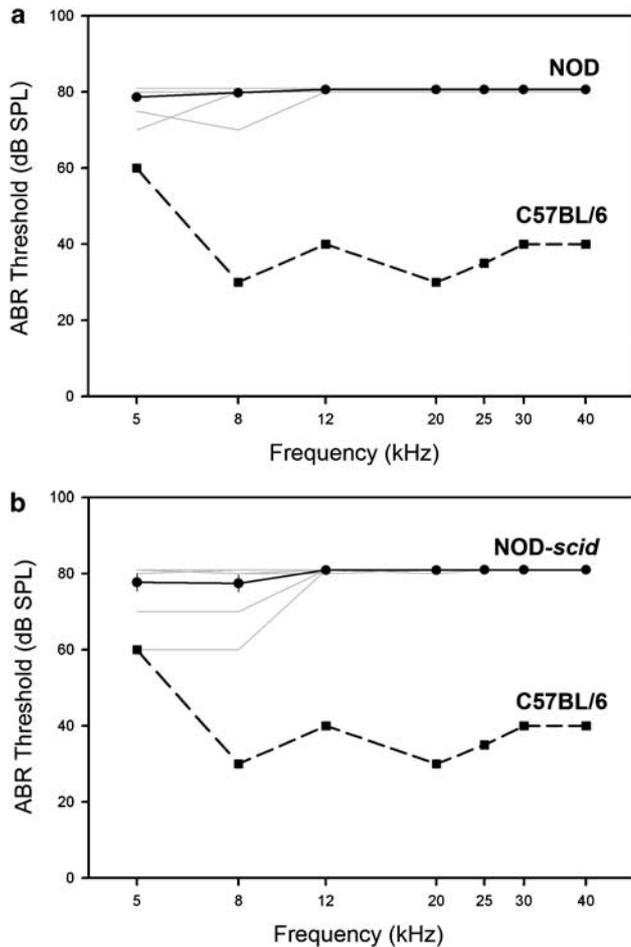
Figure 4 Characteristic audiograms for NOD and NOD-SCID mice. (**a** and **b**) Hearing function was tested electrophysiologically by measuring auditory brainstem responses (ABRs). The ABR threshold was defined as the lowest sound level at which the response peaks were clearly present. Seven frequencies were tested in the range of 5 to 40 kHz, as indicated. (**a**) ABR thresholds were measured in thirteen 5- to 8-week-old NOD animals (gray lines) and found to be high at all frequencies tested, compared to age-matched C57BL/6 control mice. The average of the results obtained with the 13 NOD animals is shown by a solid black line (NOD), with the s.e.m. indicated. (**b**) Similarly, ten young NOD-SCID animals were tested for hearing function (gray lines, average shown as a solid black line with s.e.m. indicated). All NOD-SCID animals also had high thresholds at all frequencies tested, and these results were indistinguishable from those obtained with the NOD mice. The C57BL/6 control mice were shown to exhibit low and varying thresholds at all frequencies measured (dashed lines). For individual plots, see Supplementary Figure S1a and b.

in contrast to NOD mice do not progress to either Sjogren's syndrome or diabetes without an intact immune system and therefore alteration of the immune response might have a beneficial outcome in the autoimmune host. This is not the case for the severe developmental defects in the inner ear associated with hearing loss in the NOD mouse. The *Hox11* defects in the inner ear of the NOD mouse result in severe structural abnormalities and functional hearing loss almost independent of an altered NOD immune system. Therefore, immune altering treatments of NOD mice would be predicted to aid the pancreatic and the salivary disease but not the inner ear disease. A new appreciation of the central role of altered developmental biology

in target organ dysfunction, which is either dependent or independent of immune system attack, may guide treatment strategies.

METHODS
Electrophysiological hearing test
Hearing function was tested electrophysiologically by measuring ABRs. To prepare for the ABR test, mice were anesthetized. The only surgical preparation necessary was to make a small slit in the pinna to better visualize the tympanic membrane. ABR potentials were evoked using tone pips and recorded through needle electrodes inserted through the skin (vertex to the ipsilateral pinna near the tragus with a ground electrode on the back near the tail). Stimuli were 5-ms pips. The response was amplified (×10 000), filtered (100 Hz–3 kHz), and averaged with an A–D board in a LabVIEW-driven data acquisition system. The sound pressure level (SPL) was raised in 5 dB steps from roughly 10 dB below the threshold up to 100 dB SPL. At each sound level, 1024 responses were averaged (with stimulus polarity alternated). The software average included an 'artifact reject' feature in which response waveforms were discarded if the peak-to-peak voltage exceeded 15 microV. The ABR threshold was defined as the lowest sound level at which the response peaks were clearly present and was read by eye from stacked waveforms obtained at 5 dB SPL intervals (up to 100 dB SPL). Thresholds typically corresponded to a level one step below that at which the peak-to-peak response amplitude began to rise.

Animal models
Three animal models were used in this study: non-obese diabetic (NOD), NOD-SCID and C57BL/6 mice (Taconic Laboratories, Germantown, NY, USA). NOD mice spontaneously develop two well-characterized forms of autoimmunity (that is, type 1 diabetes, from autoimmune destruction of the pancreas and Sjogren's syndrome, from autoimmune destruction of the salivary tissue). The NOD-SCID mouse model was used to track the developmental defects related to diabetes without the autoimmune condition, to effectively dissociate the immune and nonimmune factors. The NOD-SCID model is homozygous for the SCID mutation, which blocks T- and B-lymphocyte development. NOD-SCID mice are deficient in both B- and T-cell function and thus lack an adaptive immune system and have no detectable IgM, IgG1, IgG2a, IgG2b, IgG3 or IgA. NOD-SCID mice do not develop either form of autoimmunity characteristics of the parent NOD strain. The C57BL/6 mouse strain was chosen as a control strain for the NOD and NOD-SCID mice, as hearing is well characterized in C57BL/6 mice, and this strain is not known to be susceptible to autoimmune disease. Both NOD and C57BL/6 strains carry a gene (*cdh23ahl*) that gives rise to progressive age-related hearing loss with the onset after 10 months of age. For this reason, we used age-matched NOD mice and C57BL/6 mice to look for hearing loss independent of the *cdh23ah1* gene. The evaluation of hearing loss in NOD mice and NOD-SCID mice was conducted in very young animals before the onset of age-related hearing loss. All mice were housed in pathogen-free mouse facilities under the barrier protection to eliminate the effect of infection on autoimmunity and on hearing loss secondary to middle ear infections. Middle ear infections in all mice were ruled out not only by visual inspection of the middle ear for erythema and/or fluid but also by microscopic examination of middle ear tissue for signs of serous bacterial accumulation.

Harvesting and tissue preparation of the inner ear, pancreas, salivary glands and tongue
Five- to six-week-old female NOD-SCID, NOD and C57BL/6 mice (from Taconic and Jackson laboratories) were perfused through the heart with phosphate-buffered saline and a fixative solution of 10% formalin, 0.5% glutaraldehyde and 1% acetic acid. Following decapitation, the stapes was removed and the oval window punctured. Fixative was run through the oval window into the cochlea, and then the entire head was left in fixative for a week (168 h).

Before starting the embedding steps, the head was trimmed to retain a coronal section of the cochlea from both ears as well as some of the cerebrum. The tissue was then taken through following a series of embedding steps. Single washes with distilled water (DW) (15 min), 50% ethanol (15–30 min) and 70% ethanol (15–30 min) were followed by two washes with 95% ethanol

(15–30 min) and four washes with 100% ethanol (15–30 min). The sample was then incubated in 50/50 ethanol/xylene (Fisher Scientific, Pittsburgh, PA, USA) for 15 min and washed twice in xylene for 30 min each. Paraffin was then melted and held at 60 °C. The tissue was placed into a 50/50 paraffin/xylene mixture for 15 min, then washed three times for 20 min each in paraffin. The tissue was then placed into a mold with paraffin and cooled to room temperature.

Using a microtome, 7-micron sections were cut with a disposable low-profile blade (CL Sturkey, Lebanon, PA, USA). The tissue sections were put on glass plates and, using a 42 °C water bath, placed on a Fisherbrand Colorfrost/Plus Microscope Slides, Fisher Scientific, Pittsburgh, PA, USA. Before standard hematoxylin and eosin staining was performed, the slides were washed in 3-, 4- and 5-min xylene steps, placed in 100% ethanol for 5 min and 70% ethanol for 15 min and then washed in DW for 3 min. After incubating in Richard-Allan Scientific Hematoxylin I, a nuclear stain, for 5 min, slides were washed five times in DW (one DW wash cycle included washing first for a few seconds, then for 1–2 min, and then three times for a few seconds each). The slides were then placed in Richard-Allan Scientific Eosin-Y, a cytoplasmic stain, for 11 min. The slides were then subjected to a series of dehydration steps (each lasting for 1 min) in increasing concentrations of ethanol (50, 70, 80, 90 and 100%). The alcohol was then cleared in a series of xylene washes (2-, 3- and 4-min), and a coverslip (Fisherfinest Premium Cover Glass size 22×50) in a xylene-based medium (Richard-Allan Scientific Cytoseal XYL Mounting Medium, Xylene-Based) was added.

The slides were viewed with a Nikon Optiphot-2 microscope with 4× (Ph1), 10× (Ph1) and 20× (Ph2) Nikon lenses. Photographs were taken with an RT Color SPOT CCD camera manufactured by Diagnostic Instruments Inc. (Sterling Heights, MI, USA).

Three other tissue types—pancreas, salivary glands and tongue—were also studied in a manner similar to the cochlea. The tissues from 5- to 8-week-old mice were fixed, embedded, sectioned at 6 μm, and stained as described above. For the freshly harvested pancreases that were used quantitative analysis, the tissue was first teased flat before exposure to the fixative to ensure a full single fixed and cut section would display the entire pancreas from the head to tail region on a single slide. All measurements were made at a magnification of ×10 and ×100.

Quantification of pancreas, salivary gland and tongue data

At both ×10 and ×100, the size of maximum cross-area of the pancreatic islets was measured. For the analysis (in Figure 2), the islets were arbitrarily classified into three groups according to size: very small islets, medium islets and large islets. Medium islet size was determined by setting this standard relative to C57BL/6 mouse islets. A minimum of 20 islets was scored per animal on three noncontinuous pancreatic sections separated by 30 μm of cutting distance. For the estimate of the number of islets per pancreas, low power microscopic examination was used. The pancreas scored the total number of islets visible in one full cross-section of the pancreas. To ensure that one individual islet was not measured more than one time, only one scoring on one full pancreas section per mouse was performed.

Historical changes in the salivary glands were evaluated in a similar manner to the pancreas in salivary section stained with H&E. On low power ×10 magnification, followed by the examination of the sections at ×100, the sections were scored for the relative ratio of acinar to ductal tissue. We then assigned an arbitrary score compared with the control mouse acinar/duct ratios set at 1.

Quantification of histological differences between tongue sections was determined in a similar way to the pancreas and salivary glands, looking at complete cross-sections of the tongue from anterior to posterior sections. The number of fungiform and filiform papillae was counted along the superficial side of the tongue sections. Because we had determined that the number of fungiform and filiform papillae did not vary significantly between anterior and posterior sections, we averaged the number of fungiform and filiform papillae for all four sections (from anterior to posterior) for each animal. All samples were scored in a blinded fashion once the parameters for normal islet size, normal ductal to acinar ratio and normal tongue morphology were determined on age-matched control sections from C57BL/6 mice.

It should be noted that the animals presented in Figure 2 represent additional animals to the animals presented in Table 2. This is because, for quantitative analysis, the tissue needed to be prepared and embedded in paraffin in a different manner so the orientation of the tissues is identical for quantification (counting the islets, quantifying ductal tissue, and so on).

Microsoft Excel was used for statistical analyses of the salivary glands, pancreas and tongue tissue (namely, two-sample assuming equal variances *t*-test) in Figure 2e.

ABBREVIATIONS

SPL, sound pressure level; ABR, auditory brainstem responses; NOD, nonobese diabetic mouse; SCID, severe combined immunodeficiency; DW, distilled water.

ACKNOWLEDGEMENTS

1 Pelegri C, Rosmalen JG, Durant S, Throsby M, Alves V, Coulaud J *et al.* Islet endocrine-cell behavior from birth onward in mice with the nonobese diabetic genetic background. *Mol Med* 2001; **7**: 311–319.

2 Rosmalen JG, Homo-Delarche F, Durant S, Kap M, Leenen PJ, Drexhage HA. Islet abnormalities associated with an early influx of dendritic cells and macrophages in NOD and NOD-scid mice. *Lab Invest* 2000; **80**: 769–777.

3 Robinson CP, Yamamoto H, Peck AB, Humphreys-Beher MG. Genetically programmed development of salivary gland abnormalities in the NOD (nonobese diabetic)-scid mouse in the absence of detectable lymphocytic infiltration: a potential trigger for sialoadenitis of NOD mice. *Clin Immunol Immunopathol* 1996; **79**: 50–59.

4 Razavi R, Chan T, Afifiyan FN, Liu XJ, Wan X, Yantha J *et al.* TRPV1+ sensory neurons control B cell stress and islet inflammation in autoimmune diabetes. *Cell* 2006; **127**: 1123–1135.

5 Cataldo F, Marino V. Increased prevalence of autoimmune diseases in first-degree relatives of patients with celiac disease. *J Pediatr Gastroenterol Nutr* 2003; **36**: 470–473.

6 O'Leary C, Walsh CH, Wieneke P, O'Regan P, Buckley B, O'Halloran DJ *et al.* Coeliac disease and autoimmune Addison's disease: a clinical pitfall. *QJM* 2002; **95**: 79–82.

7 Zelissen PM, Bast EJ, Croughs RJ. Associated autoimmunity in Addison's disease. *J Autoimmun* 1995; **8**: 121–130.

8 Niederwieser G, Buchinger W, Bonelli RM, Berghold A, Reisecker F, Koltringer P *et al.* Prevalence of autoimmune thyroiditis and non-immune thyroid disease in multiple sclerosis. *J Neurol* 2003; **250**: 672–675.

9 Kontiainen S, Schlenzka A, Koskimies S, Rilva A, Maenpaa J. Autoantibodies and autoimmune diseases in young diabetics. *Diabetes* 1990; **13**: 151–156.

10 Park YS, Kim TW, Kim WB, Cho BY. Increased prevalence of autoimmune thyroid disease in patients with type 1 diabetes. *Korean J Intern Med* 2000; **15**: 202–210.

11 Lorini R, d'Annunzio G, Vitali L, Scaramuzza A. IDDM and autoimmune thyroid disease in the pediatric age group. *J Pediatr Endocrinol Metab* 1996; **9** (Suppl 1): 89–94.

12 Schuppan D, Hahn EG. Celiac disease and its link to type 1 diabetes mellitus. *J Pediatr Endocrinol Metab* 2001; **14** (Suppl 1): 597–605.

13 Smithson MJ. Screening for thyroid dysfunction in a community population of diabetic patients. *Diabet Med* 1998; **15**: 148–150.

14 Valentino R, Savastano S, Tommaselli AP, Dorato M, Scarpitta MT, Gigante M *et al.* Prevalence of coeliac disease in patients with thyroid autoimmunity. *Horm Res* 1999; **51**: 124–127.

15 Binder A, Maddison PJ, Skinner P, Kurtz A, Isenberg DA. Sjogren's syndrome: association with type-1 diabetes mellitus. *Br J Rheumatol* 1989; **28**: 518–520.

16 Boki KA, Ioannidis JP, Segas JV, Maragkoudakis PV, Petrou D, Adamopoulos GK *et al.* How significant is sensorineural hearing loss in primary Sjogren's syndrome? An individually matched case-control study. *J Rheumatol* 2001; **28**: 798–801.

17 Hatzopoulos S, Amoroso C, Aimoni C, Lo Monaco A, Govoni M, Martini A. Hearing loss evaluation of Sjogren's syndrome using distortion product otoacoustic emissions. *Acta Otolaryngol Suppl* 2002; **548**: 20–25.

18 Ferrer JP, Biurrun O, Lorente J, Conget JI, de Espana R, Esmatjes E *et al.* Auditory function in young patients with type 1 diabetes mellitus. *Diabetes Res Clin Pract* 1991; **11**: 17–22.

19 Fukushima H, Cureoglu S, Schachern PA, Kusunoki T, Oktay MF, Fukushima N *et al.* Cochlear changes in patients with type 1 diabetes mellitus. *Otolaryngol Head Neck Surg* 2005; **133**: 100–106.

20 Guggenheimer J, Moore PA, Rossie K, Myers D, Mongelluzzo MB, Block HM *et al.* Insulin-dependent diabetes mellitus and oral soft tissue pathologies. I. Prevalence and

characteristics of non-candidal lesions. *Oral Surg Oral Med Oral Pathol Oral Radiol Endod* 2000; **89**: 563–569.

21 Weiffenbach JM, Schwartz LK, Atkinson JC, Fox PC. Taste performance in Sjogren's syndrome. *Physiol Behav* 1995; **57**: 89–96.

22 Trune DR. Cochlear immunoglobulin in the C3H/lpr mouse model for autoimmune hearing loss. *Otolaryngol Head Neck Surg* 1997; **117**: 504–508.

23 Jabs DA, Enger C, Prendergast RA. Murine models of Sjogren's syndrome. Evolution of the lacrimal gland inflammatory lesions. *Invest Ophthalmol Vis Sci* 1991; **32**: 371–380.

24 Toda I, Sullivan BD, Rocha EM, Da Silveira LA, Wickham LA, Sullivan DA. Impact of gender on exocrine gland inflammation in mouse models of Sjogren's syndrome. *Exp Eye Res* 1999; **69**: 355–366.

25 Langenau DM, Palomero T, Kanki JP, Ferrando AA, Zhou Y, Zon LI *et al.* Molecular cloning and developmental expression of Tlx (Hox11) genes in zebrafish (Danio rerio). *Mech Dev* 2002; **117**: 243–248.

26 Logan C, Wingate RJ, McKay IJ, Lumsden A. Tlx-1 and Tlx-3 homeobox gene expression in cranial sensory ganglia and hindbrain of the chick embryo: markers of patterned connectivity. *J Neurosci* 1998; **18**: 5389–5402.

27 Patterson KD, Krieg PA. Hox11-family genes XHox11 and XHox11L2 in xenopus: XHox11L2 expression is restricted to a subset of the primary sensory neurons. *Dev Dyn* 1999; **214**: 34–43.

28 Dear TN, Colledge WH, Carlton MB, Lavenir I, Larson T, Smith AJ *et al.* The Hox11 gene is essential for cell survival during spleen development. *Development* 1995; **121**: 2909–2915.

29 Shirasawa S, Yunker AM, Roth KA, Brown GA, Horning S, Korsmeyer SJ. Enx (Hox11L1)-deficient mice develop myenteric neuronal hyperplasia and megacolon. *Nat Med* 1997; **3**: 646–650.

30 Cheng L, Arata A, Mizuguchi R, Qian Y, Karunaratne A, Gray PA *et al.* Tlx3 and Tlx1 are post-mitotic selector genes determining glutamatergic over GABAergic cell fates. *Nat Neurosci* 2004; **7**: 510–517.

31 Raju K, Tang S, Dube ID, Kamel-Reid S, Bryce DM, Breitman ML. Characterization and developmental expression of Tlx-1, the murine homolog of HOX11. *Mech Dev* 1993; **44**: 51–64.

32 Roberts CW, Sonder AM, Lumsden A, Korsmeyer SJ. Development expression of Hox11 and specification of splenic cell fate. *Am J Pathol* 1995; **146**: 1089–1101.

33 Kodama S, Davis M, Faustman DL. Diabetes and stem cell researchers turn to the lowly spleen. *Sci Aging Knowledge Environ* 2005; **2005**: pe2.

34 Dieguez-Acuna FJ, Gygi SP, Davis M, Faustman DL. Splenectomy: a new treatment option for ALL tumors expressing Hox-11 and a means to test the stem cell hypothesis of cancer in humans. *Leukemia* 2007; **21**: 2192–2194.

35 Homo-Delarche F. Is pancreas development abnormal in the non-obese diabetic mouse, a spontaneous model of type I diabetes? *Braz J Med Biol Res* 2001; **34**: 437–447.

36 Atkinson M, Gendreau P, Ellis T, Petitto J. NOD mice as a model for inherited deafness. *Diabetologia* 1997; **40**: 868.

37 Virtaniemi J, Laakso M, Nuutinen J, Karjalainen S, Vartiainen E. Tympanometry in patients with insulin-dependent diabetes mellitus. *Scand Audiol* 1993; **22**: 217–222.

38 Miyagawa JI, Hanafusa T, Miyazaki A, Yamada K, Fujino-Kurihara H, Nakajima H *et al.* Ultrastructural and immunocytochemical aspects of lymphocytic submandibulitis in the non-obese diabetic (NOD) mouse. *Virchows Arch* 1986; **51**: 215–225.

39 Rulifson EJ, Kim SK, Nusse R. Ablation of insulin-producing neurons in flies; growth and diabetic phenotypes. *Science* 2002; **296**: 1118–1120.

40 Salomon B, Rhee L, Bour-Jordan H, Hsin H, Montag A, Soliven B *et al.* Development of spontaneous autoimmune peripheral polyneuropathy in B7-2-deficient NOD mice. *J Exp Med* 2001; **194**: 667–684.

41 Setoguchi R, Hori S, Takahashi T, Sakaguchi S. Homeostatic maintenance of natural Foxp3(+)CD25(+) CD4(+) regulatory T cells by interleukin (IL)-2 and induction of autoimmune disease by IL-2 neutalization. *J Exp Med* 2005; **201**: 723–735.

42 Cheng L, Arata A, Mizuguchi R, Qian Y, Karunaratne A, Gray PA *et al.* Tlx3 and Tlx1 are post-mitotic selector genes determining glutamatergic over GABAergic cell fates. *Nat Neurosci* 2004; **7**: 510–517.